On the background estimation by time slides in a network of gravitational wave detectors

Michal Was, Marie-Anne Bizouard, Violette Brisson, Fabien Cavalier, Michel Davier, Patrice Hello, Nicolas Leroy, Florent Robinet, Vavoulidis Miltiadis

On the background estimation by time slides in a network of gravitational wave detectors

Michał Wąs, Marie-Anne Bizouard, Violette Brisson, Fabien Cavalier, Michel Davier, Patrice Hello, Nicolas Leroy, Florent Robinet and Miltiadis Vavoulidis.

LAL, Univ Paris-Sud, CNRS/IN2P3, Orsay, France.

E-mail: mwas@lal.in2p3.fr

Abstract. Time shifting the outputs of Gravitational Wave detectors operating in coincidence is a convenient way to estimate the background in a search for short duration signals. However this procedure is limited as increasing indefinitely the number of time shifts does not provide better estimates. We show that the false alarm rate estimation error saturates with the number of time shifts. In particular, for detectors with very different trigger rates this error saturates at a large value. Explicit computations are done for 2 detectors, and for 3 detectors where the detection statistic relies on the logical "OR" of the coincidences of the 3 couples in the network.

PACS numbers: 04.80.Nm, 07.05.K

1. Introduction

Kilometric interferometric Gravitational Wave (GW) detectors such as LIGO [1] or Virgo [2] have been taking data with increasing sensitivities over the past years [3, 4, 5, 6, 7, 8, 9]. It is expected that short duration GW events, e.g. the so-called bursts emitted by gravitational collapses or the signals emitted by compact binary inspirals, are very rare. Moreover the output of the detectors is primarily (non Gaussian) noise, and this background noise is in general not modeled. This implies that with a single GW detector it is very difficult to estimate the background event rate, and then to assess the significance of some GW candidate.

On the contrary when dealing with a network of detectors (that means in practice at least two detectors of the same class), there is a conventional and simple way to estimate the background, that is the rate of coincident events due to detector noise. This consists of time shifting the search algorithm outputs (or triggers) of each detector with respect to the other(s), by some unphysical delays, much larger than the light travel time between the detectors and much larger than the typical duration of an expected GW signal. The next step is then to look for coincidences between shifted triggers just as if the shifted streams were synchronized. As we deal with *a priori* rare events, we need to set in practice low false alarm rates in the analysis. The question then arises of how many time slides are needed for correctly estimating the background and especially its tails where rare (non-Gaussian noise) events lay. Note, that in practice in burst or binary inspiral searches, a hundred or more time slides are done [3, 6, 7], due in particular to limited computational resources. Such a limitation of course depends on the duration of the different detectors data streams and on the complexity of consistency tests performed on coincident triggers. For example, time slides computation for one year of data sampled at 16384 Hz (LIGO) or 20 kHz (Virgo) can rapidly become a computational burden, especially when computationally intensive consistency tests like the χ^2 veto [10] are used.

In this paper, we show that the precision on the background estimation, using time slides of trigger streams, is in fact limited. Indeed the variance of the false alarm rate estimation does not indefinitely decrease as the number of time slides increases as we would naively believe. On the contrary this variance saturates at some point, depending on the trigger rates chosen in each individual detector and on the coincidence time window set for identifying coincident events in the network of detectors.

After introducing the general definitions in section 2, we give explicit formulas for the two-detector and the three-detector case in respectively Sec. 3 and 4. In the latter we restrict ourselves to the particular analysis scheme where we are looking at the union (logical "OR") of the three couples of detectors. This is actually the configuration of interest, since it is more sensitive than simply searching for triple coincidences (logical "AND") [11]. In each case (2 or 3 detectors) we check the analytical result with a Monte Carlo simulation and find excellent agreement. In section 5 these results are applied and discussed using typical parameters of a GW data analysis.

2. Definitions

2.1. Poisson approximation for trigger generation

Background triggers in the detectors are due to rare glitches. Often these glitches come in groups, but most analysis pipelines cluster their triggers, so each glitch group results in only one final trigger. This clustering procedure is reasonable as long as the resulting trigger rate is much lower than the inverse of the typical clustering time length. In this limit the clustered triggers are independent events. Thus, throughout this paper we will assume that each detector produces random background triggers, which are Poisson distributed in time.

2.2. Problem description

We look then at the coincidence between two Poisson processes. The single interferometer trigger rate will be noted FA_1, FA_2, ..., the coincidence rate will be simply noted FA. We denote by $\widetilde{\mathrm{FA}}(\mathcal{T})$ the rate resulting from counting the number of coincidence between two data streams, that are shifted by some time $\mathcal{T}$. In particular for zero lag ($\mathcal{T} = 0$) the measured rate is $\widetilde{\mathrm{FA}}(0)$. So the quantities with tildes are the experimentally measured rates, and the quantities without tildes are the actual Poisson distribution parameters. The purpose of the paper is to study the properties of the time shifting method, which uses $\widehat{\mathrm{FA}} = \frac{1}{R}\sum_{k=1}^{R} \widetilde{\mathrm{FA}}(\mathcal{T}_k)$ as an estimator of FA, where R is the number of time slides and $\mathcal{T}_k$ is the k^{th} time slide stride.

2.3. Poisson process model

To model a Poisson process with event rate FA_1 we discretize the data stream duration T with bins of length Δt, the discretization time scale, e.g. either the detector sampling rate or the clustering time scale. Thus, for each bin an event is present with a probability $p = \mathrm{FA}_1 \Delta t$ ‡.

To ease the calculation we describe the Poisson process realizations with a continuous random variable. We take $\boldsymbol{x}$ uniformly distributed in the volume $[0,1]^N$ where $N = \frac{T}{\Delta t}$ is the number of samples, then compare x_k (the k^{th} coordinate of $\boldsymbol{x}$) with p. When $x_k < p$ there is an event in time bin k, otherwise there is none. Thus $\boldsymbol{x}$ characterizes one realization of a Poisson process, and it can be easily seen that the uniform distribution of $\boldsymbol{x}$ leads to a Poisson distribution of events.

2.4. Coincidences

We choose the sampling Δt to be equal to twice the coincidence time window τ_c, in order to simplify the modeling of the coincidence between two processes. More precisely, for two Poisson processes with event rates respectively FA_1 and FA_2, we define a coincidence

‡ Here we model the Poisson process by a binomial distribution, recalling that when $p \ll 1$ the binomial distribution tends toward a Poisson distribution

when there is an event in the same time bin k for both processes. This is different from the usual definition, where events are said in coincidence when they are less than a time window apart. This binning time coincidence has on average the same effects as defining as coincident events that are less than $\pm\frac{1}{2}\Delta t = \pm\tau_c$ apart. The analytical results are derived using this non standard definition, but they are in precise agreement with Monte Carlo simulations that are performed using the usual definition of time coincidence.

3. The case of two detectors

3.1. Time slides between two detectors

Let $\boldsymbol{x}, \boldsymbol{y} \in [0,1]^N$ be two realizations of Poisson processes with respectively $p = \mathrm{FA}_1\Delta t$ and $q = \mathrm{FA}_2\Delta t$. There is a coincident event in time bin k when $x_k < p$ and $y_k < q$. So the total number of coincidences for this realization is

$$\sum_{k=1}^{N} \mathbb{1}(x_k < p)\mathbb{1}(y_k < q) \tag{1}$$

where

$$\begin{cases} \mathbb{1}(a) = 1 & \text{if } a \text{ is true} \\ \mathbb{1}(a) = 0 & \text{if } a \text{ is false} \end{cases} \tag{2}$$

Thus the mean number of coincidences without time slides is as expected

$$\text{Mean} = \int_{x_1}\cdots\int_{x_N}\int_{y_1}\cdots\int_{y_N}\sum_{k=1}^{N}\mathbb{1}(x_k < p)\mathbb{1}(y_k < q)\underbrace{\mathrm{d}x_1\cdots\mathrm{d}x_N\mathrm{d}y_1\cdots\mathrm{d}y_N}_{\mathrm{d}V} = Npq. \tag{3}$$

To consider a number R of time slides we take a set of R circular permutations of $[\![1, N]\!]$. Time-sliding a vector $\boldsymbol{x}$ by the circular permutation π transforms the vector $\boldsymbol{x}$ into the vector of coordinates $x_{\pi(k)}$. Then the mean number of coincidences is simply

$$\text{Mean} = \int_{x_1}\cdots\int_{x_N}\int_{y_1}\cdots\int_{y_N}\frac{1}{R}\sum_{\pi}\sum_{k}\mathbb{1}(x_k < p)\mathbb{1}(y_{\pi(k)} < q)\mathrm{d}V = Npq, \tag{4}$$

thus there is no bias resulting from the use of time slides.

3.2. Computation of the variance

In order to have an estimate of the statistical error, we compute the variance with R time slides. The second moment is

$$\begin{aligned} \mathrm{M}_2 &= \int_{x_1}\cdots\int_{x_N}\int_{y_1}\cdots\int_{y_N}\left[\frac{1}{R}\sum_{\pi}\sum_{k}\mathbb{1}(x_k < p)\mathbb{1}(y_{\pi(k)} < q)\right]^2\mathrm{d}V \\ &= \int\cdots\int\frac{1}{R^2}\sum_{\pi_1}\sum_{\pi_2}\sum_{k}\sum_{l}\mathbb{1}(x_k < p)\mathbb{1}(x_l < p)\mathbb{1}(y_{\pi_1(k)} < q)\mathbb{1}(y_{\pi_2(l)} < q)\mathrm{d}V. \end{aligned} \tag{5}$$

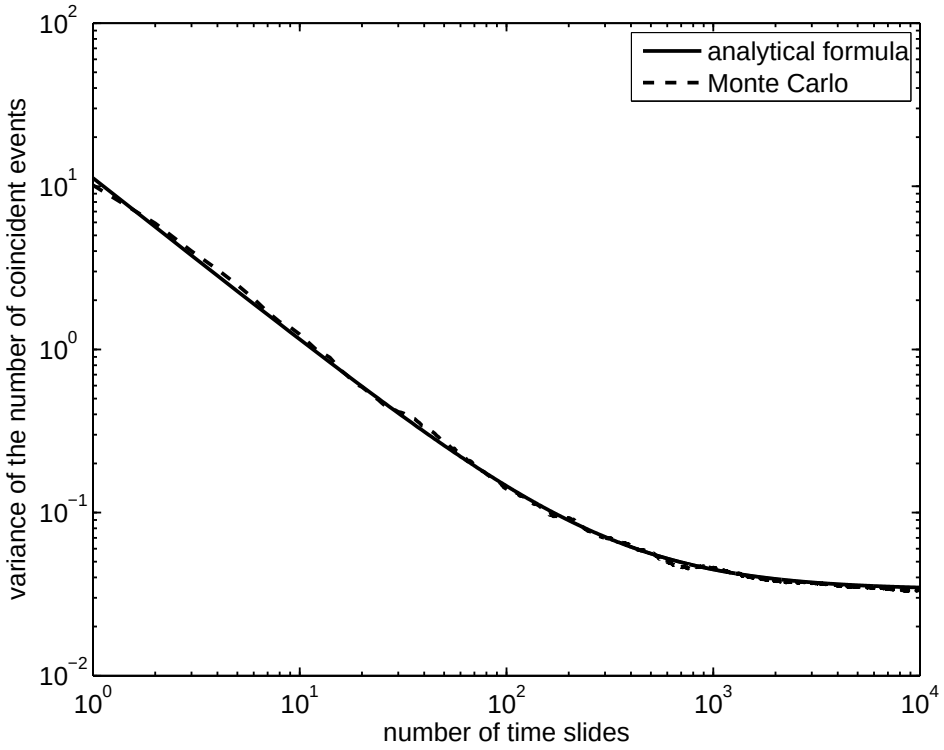

Figure 1. The solid line is the analytical formula (7) of the variance and the dashed line is the Monte Carlo variance as a function of the number of times slides. The Monte Carlo has been performed with $\mathrm{FA}_1 = 0.7\,\mathrm{Hz}$, $\mathrm{FA}_2 = 0.8\,\mathrm{Hz}$, $\tau_c = 1\,\mathrm{ms}$, 500 trials and a $T = 10^4\,\mathrm{s}$ data stream length.

We can then exchange integrals and sums. To compute the integrals we distinguish two cases: when $k \neq l$ the integrals on x_k and x_l are independent, and the integration over $x_1, \ldots, x_N$ gives a p^2 contribution; otherwise the integration gives a p contribution. Analogously for the y variables we obtain q or q^2 depending on whether $\pi_1(k) = \pi_2(l)$ or not.

The computation of this integral, detailed in Appendix A, yields

$$\mathrm{Var} = Npq\left[\frac{1}{R} + p + q + \frac{pq - (p+q)}{R} - 2pq\right] \tag{6}$$

$$\simeq Npq\left[\frac{1}{R} + p + q\right], \tag{7}$$

where the last line is an approximation in the limit p, q, $\frac{1}{R} \ll 1$, which is reasonable as far as GW analysis is concerned.

3.3. Interpretation

Each term in equation (7) can be interpreted. The $\frac{1}{R}$ is what we would expect if we considered R independent Poisson process realizations instead of R time slides. The $p+q$ comes from the estimation of the Poisson process event rate. Indeed, the estimation

of the event probability p from a single realization of a Poisson process with a mean number of events Np is $\widehat{p} = p + \delta p$, where δp is the random statistical error with variance $\langle \delta p^2 \rangle = \frac{p}{N}$. This yields the mean rate of coincidences

$$\text{Mean} = N\widehat{p}\widehat{q} = N\left(p + \delta p\right)\left(q + \delta q\right) \simeq Npq + Np\delta q + Nq\delta p \tag{8}$$

which corresponds to a variance of $\langle N^2 p^2 \delta q^2 + N q^2 \delta p^2 \rangle = Npq(p+q)$, because δp and δq are independent errors. Thus, when using only one realization for the single detector triggers, we have a statistical error on the single detector process rate. This statistical error is systematically propagated to the coincidence rate of each time slide, that yields the extra terms in the variance as compared to independent process realizations. One can see that this extra term is important when $\frac{1}{R} < \max(p, q)$; for cases where the coincident false alarm rate is maintained fixed (pq constant), the effect is most noticeable when p and q are very different.

This gives an estimate of the variance of the number of coincident events in a data stream of length T. After converting to the estimation of the coincidence false alarm rate we obtain

$$\text{Mean}_{\widehat{\text{FA}}} = \frac{\text{Mean}}{T} = \text{FA}_1\text{FA}_2\Delta t, \tag{9}$$

$$\text{Var}_{\widehat{\text{FA}}} = \frac{\text{Var}}{T^2} \simeq \text{FA}_1\text{FA}_2\frac{\Delta t}{T}\left[\frac{1}{R} + \text{FA}_1\Delta t + \text{FA}_2\Delta t\right]. \tag{10}$$

To verify these results, a Monte Carlo simulation has been performed. The Poisson processes are created as described in section 2, using a sampling rate of 16384 Hz, then a simple coincidence test with a window of $\tau_c = 1\,\text{ms}$ is applied. The time shifts are done by adding an integer number of seconds to all events and applying a modulo T operation. The formula has been tested using 500 realizations of $T = 10^4\,\text{s}$ long Poisson processes, and using between 1 and 10^4 time slides for each realization. Figure 1 shows that the analytical formula (7) and the Monte Carlo agree well for any number of time slides, and that the variance starts saturating when a few hundred time slides are used. We can see that the identification of the sampling time and the coincidence time window has no consequence on the result, the choice between binning and windowing the coincidences is a higher order effect.

3.4. Straightforward extensions of the model

In real data analysis, there are times when one of the detectors does not take science quality data for technical reasons. Thus, the data set is divided into disjoint segments, and the background estimation is often done by circular time slides on each segment separately. Afterwards the results from all the segments are combined to get the background false alarm estimation. The computation discussed above extends to this case with minimal changes. The circular permutations have to be changed to circular by block permutations, everything else being kept identical.

Another caveat is that for real data analysis the coincidence procedure is often more complicated. Some of those complications are event consistency tests, e.g. do the two coincident events have a similar frequency? We can model this by adding some parameter f distributed uniformly in $[0, 1]$ attached to each event, and then requesting a coincidence in the parameter f.

For this model the results will be the same as those above, up to a factor of order 1. Indeed, instead of applying a window of size Δt to our events, we are now working in a 2 dimensional (for instance time-frequency) space and using a rectangular window in this 2D parameter space. The procedure in both cases is the same — applying D dimensional rectangular windows to events distributed uniformly in a D dimensional space — up to the dimension of the space.

4. The case of three detectors

4.1. Time slides between three detectors

In the case of three detectors one natural extension is to ask for events that are seen by at least two detectors, which means look for coincidence between two detectors for each detector pair, but counting the coincidences between three detectors only once. This "OR" strategy in a interferometer network has been shown to be more efficient than a direct three fold coincidence strategy ("AND" strategy) [11]. For time slides, when shifting the events of the second detector with some permutation π, we also shift the events of the third detector by the same amount but in the opposite direction with π^{-1}. To write compact equations we abbreviate $X = \mathbb{1}(x_k < p)$, $Y = \mathbb{1}(y_{\pi(k)} < q)$, $Z = \mathbb{1}(z_{\pi^{-1}(k)} < r)$, $\mathrm{d}V = \mathrm{d}x_1 \cdots \mathrm{d}x_N \mathrm{d}y_1 \cdots \mathrm{d}y_N \mathrm{d}z_1 \cdots \mathrm{d}z_N$, where $r = \mathrm{FA}_3 \Delta t$ is the event probability per bin of the third detector and the vector $\boldsymbol{z}$ describes its realizations. Thus, the mean number of coincidences in the framework described in section 3.1 is

$$\mathrm{Mean} = \int \cdots \int \frac{1}{R} \sum_{\pi} \sum_{k} \left[XY + YZ + XZ - 2XYZ\right] \mathrm{d}V = N\left[pq + pr + qr - 2pqr\right]. \tag{11}$$

4.2. Computation of the variance

The second moment can be written compactly as

$$\begin{aligned} \mathrm{M}_2 = \int \cdots \int \frac{1}{R^2} \sum_{\pi_1} \sum_{\pi_2} \sum_{k} \sum_{l} \\ \left[XYX'Y' + XZX'Z' + YZY'Z' + 4XYZX'Y'Z' + 2XYX'Z' + 2XYY'Z' \right. \\ \left. + 2XZY'Z' - 4XYX'Y'Z' - 4XZX'Y'Z' - 4YZX'Y'Z'\right] \mathrm{d}V, \end{aligned} \tag{12}$$

where the $'$ denotes whether the hidden variables are π_1, k or π_2, l.

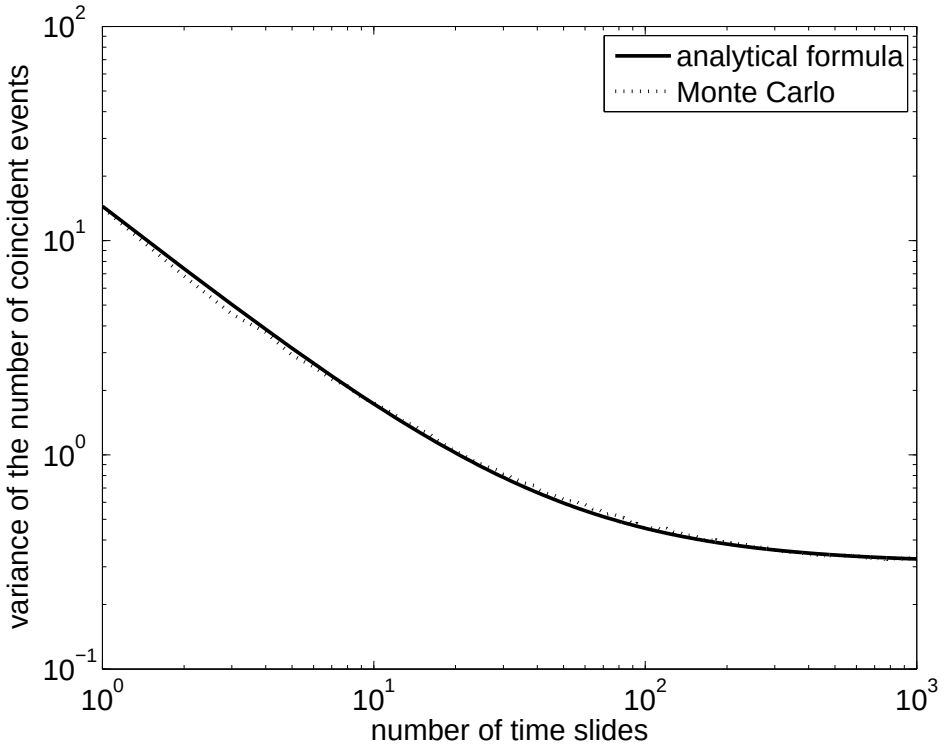

Figure 2. The solid line is the analytical formula (14) of the variance and the dotted line is the Monte Carlo variance as a function of the number of time slides. The Monte Carlo has been performed with $\mathrm{FA}_1 = 0.04\,\mathrm{Hz}$, $\mathrm{FA}_2 = 0.08\,\mathrm{Hz}$, $\mathrm{FA}_3 = 0.16\,\mathrm{Hz}$, $\tau_c = 31\,\mathrm{ms}$, 500 trials and a $T = 10^4\,\mathrm{s}$ data stream length.

The computation of this integral, detailed in Appendix B, yields

$$\begin{aligned}\mathrm{M}_2 = \frac{N}{R}\Big\{&(pq+pr+qr-2pqr)\\ &+(R-1)\left[pq(p+q+pq)+pr(p+r+pr)+qr(q+r+qr)+6pqr-4pqr(p+q+r)\right]\\ &+\left[(R-1)(N-3)+(N-1)\right](pq+pr+qr-2pqr)^2\Big\},\end{aligned} \quad (13)$$

and can be approximated in the limit $p, q, r, \frac{1}{R} \ll 1$ by

$$\mathrm{Var} \simeq N(pq+pr+qr)\left(\frac{1}{R}+p+q+r+\frac{3pqr}{pq+pr+qr}\right). \quad (14)$$

4.3. Interpretation

Similarly to section 3.3 the extra terms in equation (14) can be explained through the error in the estimation of the single detector event rate. Using the same notations as in section 3.3 the mean coincidence number is

$$\mathrm{Mean} = N\left(\hat{p}\hat{q}+\hat{p}\hat{r}+\hat{q}\hat{r}\right) \simeq N\left[pq+pr+qr+(q+r)\delta p+(p+r)\delta q+(p+q)\delta r\right]. \quad (15)$$

Using the independence of estimation errors and recalling that $\langle \delta p^2 \rangle = \frac{p}{N}$ we obtain the variance of this mean value

$$\begin{aligned} \mathrm{Var} &= N^2 \left[\langle \delta p^2 \rangle (q+r)^2 + \langle \delta q^2 \rangle (p+r)^2 + \langle \delta r^2 \rangle (p+q)^2 \right] \\ &= N \left[(pq+pr+qr)(p+q+r) + 3pqr \right], \end{aligned} \tag{16}$$

that corresponds to the extra terms in equation (14).

After converting to the estimation of the false alarm rate we obtain

$$\mathrm{Mean}_{\widehat{\mathrm{FA}}} \simeq (\mathrm{FA}_1\mathrm{FA}_2 + \mathrm{FA}_1\mathrm{FA}_3 + \mathrm{FA}_2\mathrm{FA}_3)\Delta t, \tag{17}$$

$$\begin{aligned} \mathrm{Var}_{\widehat{\mathrm{FA}}} \simeq\ & (\mathrm{FA}_1\mathrm{FA}_2 + \mathrm{FA}_1\mathrm{FA}_3 + \mathrm{FA}_2\mathrm{FA}_3)\frac{\Delta t}{T} \\ & \left(\frac{1}{R} + \mathrm{FA}_1\Delta t + \mathrm{FA}_2\Delta t + \mathrm{FA}_3\Delta t + \frac{3\mathrm{FA}_1\mathrm{FA}_2\mathrm{FA}_3}{\mathrm{FA}_1\mathrm{FA}_2 + \mathrm{FA}_1\mathrm{FA}_3 + \mathrm{FA}_2\mathrm{FA}_3}\Delta t \right). \end{aligned} \tag{18}$$

To check the 3 detector results we performed a Monte Carlo similar to the one of the 2 detector case (see section 3.3). The only difference is the number of detectors, and we choose a different coincidence window: $\tau_c = 31\,\mathrm{ms}$ §. To check that the assumption of equal and opposite time slides does not influence the result, in the Monte Carlo the data in the second detector are shifted by $\mathcal{T}_k$ and in the third detector by $3\mathcal{T}_k$. Figure 2 shows that the Monte Carlo and the 3 detector "OR" formula (14) agree really well.

4.4. The case of D detectors

For the sake of completeness we can generalize the interpretation done in section 3.3 to the case of D detectors in the "AND" configuration. This generalization of equation (8) to D detectors yields a variance on the number of coincidences

$$\mathrm{Var} \simeq N \prod_{i=1}^{D} p_i \left(\frac{1}{R} + \sum_{i=1}^{D} \prod_{j \neq i} p_j \right), \tag{19}$$

where p_i is the probability for detector i to have an event in a given time bin.

The interpretation can also be generalized in the "OR" case, that is coincidence between any pair of detectors, although the computation is more cumbersome as detailed in Appendix C and yields

$$\mathrm{Var} \simeq N \left[\left(\sum_{i<j} p_i p_j \right) \left(\frac{1}{R} + \sum_{i=1}^{D} p_i \right) + \frac{1}{2} \sum_{i \neq j,\, j \neq k,\, k \neq i} p_i p_j p_k \right], \tag{20}$$

where p_i is the event probability per bin in the i$^{\mathrm{th}}$ detector.

§ This accounts for the largest light travel time in the LIGO-Virgo network (27 ms) and some timing error in each detector.

5. Discussion

We finally discuss the consequences of the above results on GW data analysis. To be able to put numbers into the equations we will look at a fiducial GW data taking run. We choose the run properties to be:

- a duration of $T = 10^7\,\mathrm{s}$, that is roughly 4 months
- two detectors with a light travel time separation of 25 ms, and we use the same time as the coincidence window, so that $\Delta t = 50\,\mathrm{ms}$‖, assuming perfect timing accuracy of trigger generators.
- a desired coincidence false alarm rate of $10^{-8}\,\mathrm{Hz}$, i.e. one event every three years.

We will look at two special cases of single detector threshold choice. One symmetric case, where thresholds are set so that the single detector trigger rate in each detector is roughly the same. One asymmetric case, where in one of the detectors there is only one trigger. This asymmetric case is extreme but instructive, because tuning the thresholds to obtain the best sensitivity often yields asymmetric trigger rates between different detectors.

Symmetric detector case In this case we have the single detector trigger rate $\mathrm{FA}_1 = \mathrm{FA}_2 = \mathrm{FA}_s = \sqrt{\frac{\mathrm{FA}}{\Delta t}} \simeq 4.5 \times 10^{-4}\,\mathrm{Hz}$, which gives using equation (10) the fractional error of the false alarm estimation

$$\begin{aligned} \frac{\sigma_{\mathrm{FA}}}{\mathrm{FA}} &\simeq 3.2 \left(\frac{1}{R} + 4.5 \times 10^{-5} \right)^{\frac{1}{2}} && p = q = 2.25 \times 10^{-5} \\ &\simeq 0.32 && \text{for } R = 100 \\ &\simeq 0.02 && \text{for } R \to \infty. \end{aligned}$$

So for 100 time slides we get a typical error of 30% in the false alarm estimation, and the error saturates at 2% for $R \gtrsim 20000$.

Asymmetric detector case In this extreme case the single detector trigger rates are $\mathrm{FA}_1 = \frac{1}{T} = 10^{-7}\,\mathrm{Hz}$ and $\mathrm{FA}_2 = \frac{\mathrm{FA}}{\mathrm{FA}_1 \Delta t} = 2\,\mathrm{Hz}$, which gives using equation (10) the fractional error of the false alarm estimation

$$\begin{aligned} \frac{\sigma_{\mathrm{FA}}}{\mathrm{FA}} &\simeq 3.2 \left(\frac{1}{R} + 0.1 \right)^{\frac{1}{2}} && p = 5 \times 10^{-9},\ q = 0.1 \\ &\simeq 1.05 && \text{for } R = 100 \\ &\simeq 1 && \text{for } R \to \infty. \end{aligned}$$

So the error saturates at 100%, and this saturation is achieved for $R \gtrsim 10$.

Those two examples show that the maximal number of useful time slides and the false alarm estimation precision strongly depends on the relative properties of the two

‖ As noted in section 2.4, coincident triggers are defined as less that $\pm\frac{1}{2}\Delta t$ apart.

detectors. In particular when there are much more triggers in one detector than in the other, the background can be badly estimated and increasing the number of time slides does not solve the issue.

6. Conclusions

We have studied the statistical error in the background estimation of event-based GW data analysis when using the time slide method. Under the assumption of stationary noise we analytically computed this error in both the two-detector and three-detector case, and found excellent agreement with Monte Carlo simulations.

The important resulting consequences are: the precision on the background estimation saturates as a function of the number of time slides, this saturation is most relevant for detectors with a very different trigger rate where the background estimation precision can be poor for any number of time slides.

Let us note that the time slide method can be used in other situations than GW data background estimation. For example it can be used to estimate the rate of accidental coincidences between a GW channel and an environmental channel in a GW interferometer; or in any experiment where coincidences between two (or more) trigger generators are looked for. The results of this paper can be straightforwardly extended to such an experiment.

Another limitation, the non stationarity of the data, has not been investigated in this paper. Data non stationarity is a well known issue in GW data analysis [12]. In the context of the time slides method it raises the question whether the time shifted data are still representative of the zero lag data, when large time shifts are used. It involves both the problem of the measure of the level of data non stationarity, and the estimation of the error it induces on the background estimation. Further work on this issue will be the subject of a future paper.

Appendix A. Two-detector integral

To compute the integral

$$\begin{aligned} \mathrm{M}_2 &= \int_{x_1}\cdots\int_{x_N}\int_{y_1}\cdots\int_{y_N}\left[\frac{1}{R}\sum_{\pi}\sum_{k}\mathbb{1}(x_k<p)\mathbb{1}(y_{\pi(k)}<q)\right]^2 \\ &= \int\cdots\int\frac{1}{R^2}\sum_{\pi_1}\sum_{\pi_2}\sum_{k}\sum_{l}\mathbb{1}(x_k<p)\mathbb{1}(x_l<p)\mathbb{1}(y_{\pi_1(k)}<q)\mathbb{1}(y_{\pi_2(l)}<q), \quad \text{(A.1)} \end{aligned}$$

we put the sums outside the integrals. When $k \neq l$, the integrals on x_k and x_l are independent, and the integration over $x_1, \ldots, x_N$ gives a p^2 contribution. Otherwise the integration gives a p contribution. Analogously for the y variables we get q^2 or q depending on whether $\pi_1(k) \neq \pi_2(l)$ or not.

Thus we get four types of integrals

$$\text{integral} \times \text{number of such integrals}$$

$$k = l, \pi_2^{-1} \circ \pi_1(k) = l \qquad \frac{1}{R^2} pq \times NR \tag{A.2a}$$

$$k \neq l, \pi_2^{-1} \circ \pi_1(k) = l \qquad \frac{1}{R^2} p^2 q \times NR(R-1) \tag{A.2b}$$

$$k = l, \pi_2^{-1} \circ \pi_1(k) \neq l \qquad \frac{1}{R^2} pq^2 \times NR(R-1) \tag{A.2c}$$

$$k \neq l, \pi_2^{-1} \circ \pi_1(k) \neq l \qquad \frac{1}{R^2} p^2 q^2 \times N\left[R(R-1)(N-2) + R(N-1)\right] \tag{A.2d}$$

Here we used that the composition of two circular permutation is a circular permutation, and that the only circular permutation with a fixed point is the identity.

The details of the combinatorics are as follows.

- $k = l, \pi_2^{-1} \circ \pi_1(k) = l$: There are N different k values. For each of them there is only one l that is equal to it. Here $\pi_2^{-1} \circ \pi_1$ is a circular permutation with a fixed point, so it is the identity. There are R different π_1, and for each of them only $\pi_2 = \pi_1$ gives the identity.
- $k \neq l, \pi_2^{-1} \circ \pi_1(k) = l$: There are N different k values. For every pair $\pi_1 \neq \pi_2$ we get $\pi_1^{-1} \circ \pi_2(k) \neq k$. And the choice of this pair determines uniquely an l that is not equal to k. There are $R(R-1)$ such pairs.
- $k = l, \pi_2^{-1} \circ \pi_1(k) \neq l$: There are N different k values. The value of l is determined by the equality $k = l$. And there are $R(R-1)$ pairs of π_1, π_2 such that $\pi_1^{-1} \circ \pi_2(k) \neq k$.
- $k \neq l, \pi_2^{-1} \circ \pi_1(k) \neq l$: There are N different k values. In the case where $\pi_1 \neq \pi_2$, we need that $l \neq k$ and $l \neq \pi_2^{-1} \circ \pi_1(k)$, there are $N-2$ such l. In the case where $\pi_1 = \pi_2$ we get $k = \pi_2^{-1} \circ \pi_1(k)$, so there is only one inequality on l, and there are $N-1$ possible l.

By summing the 4 terms above and subtracting Mean^2 we obtain

$$\text{Var} = \frac{1}{R} Npq\left[1 + p(R-1) + q(R-1) + pq\big((R-1)(N-2) + (N-1)\big)\right] - (Npq)^2 \tag{A.3}$$

$$= Npq\left[\frac{1}{R} + p + q + \frac{pq - (p+q)}{R} - 2pq\right] \tag{A.4}$$

$$\simeq Npq\left[\frac{1}{R} + p + q\right], \tag{A.5}$$

Appendix B. Three-detector integral

We want to compute the integral

$$\mathrm{M}_2 = \int\cdots\int \frac{1}{R^2}\sum_{\pi_1}\sum_{\pi_2}\sum_{k}\sum_{l} [XYX'Y' + XZX'Z' + YZY'Z' + 4XYZX'Y'Z' + 2XYX'Z' + 2XYY'Z' + 2XZY'Z' - 4XYX'Y'Z' - 4XZX'Y'Z' - 4YZX'Y'Z'], \quad \text{(B.1)}$$

where the $'$ denotes whether the hidden variables are π_1, k or π_2, l.

Similarly to Appendix A we have here eight kind of integrals.

X	Y	Z	number of such integrals
$k=l,$	$\pi_2^{-1}\circ\pi_1(k)=l,$	$\pi_2\circ\pi_1^{-1}(k)=l,$	NR
$k=l,$	$\pi_2^{-1}\circ\pi_1(k)=l,$	$\pi_2\circ\pi_1^{-1}(k)\neq l,$	0
$k=l,$	$\pi_2^{-1}\circ\pi_1(k)\neq l,$	$\pi_2\circ\pi_1^{-1}(k)=l,$	0
$k=l,$	$\pi_2^{-1}\circ\pi_1(k)\neq l,$	$\pi_2\circ\pi_1^{-1}(k)\neq l,$	$NR(R-1)$
$k\neq l,$	$\pi_2^{-1}\circ\pi_1(k)=l,$	$\pi_2\circ\pi_1^{-1}(k)=l,$	0
$k\neq l,$	$\pi_2^{-1}\circ\pi_1(k)=l,$	$\pi_2\circ\pi_1^{-1}(k)\neq l,$	$NR(R-1)$
$k\neq l,$	$\pi_2^{-1}\circ\pi_1(k)\neq l,$	$\pi_2\circ\pi_1^{-1}(k)=l,$	$NR(R-1)$
$k\neq l,$	$\pi_2^{-1}\circ\pi_1(k)\neq l,$	$\pi_2\circ\pi_1^{-1}(k)\neq l,$	$NR\left[(R-1)(N-3)+(N-1)\right]$

In these combinatoric computations we need to assume that all translations are smaller than $N/4$, to ensure that $\pi_2^{-1}\circ\pi_1\circ\pi_2^{-1}\circ\pi_1(k)=k \Rightarrow \pi_1=\pi_2$. This assumption is really reasonable, and the result would not be significantly different without it.

The final result is

$$\mathrm{M}_2 = \frac{N}{R}\Big\{(pq+pr+qr-2pqr) + (R-1)\left[pq(p+q+pq)+pr(p+r+pr)+qr(q+r+qr)+6pqr-4pqr(p+q+r)\right] + \left[(R-1)(N-3)+(N-1)\right](pq+pr+qr-2pqr)^2\Big\}, \quad \text{(B.2)}$$

Appendix C. "OR" case for D detectors

Using the same heuristic as in section 3.3 and 4.3 we compute the variance of the time slide estimation method for D detectors in the "OR" case. This heuristic yielded the same results as the exact computation for the 2 and 3 detector case, thus we may expect it to stay true in the general case.

As in equation (14), the variance is the sum of the normal Poisson variance

$$\mathrm{Var}_{\mathrm{Poiss}} = N\left(\sum_{j=1}^{D}\sum_{i=1}^{j-1} p_i p_j\right)\frac{1}{R}, \quad \text{(C.1)}$$

and the variance due to time slides.

The estimate of the mean rate is

$$\text{Mean} = N \left[\sum_{j=1}^{D} \sum_{i=1}^{j-1} (p_i + \delta p_i)(p_j + \delta p_j) \right] \tag{C.2}$$

$$\simeq N \left[\sum_{j=1}^{D} \sum_{i=1}^{j-1} p_i p_j + \sum_{j=1}^{D} \delta p_j \left(\sum_{\substack{i=1 \\ i \neq j}}^{D} p_i \right) \right], \tag{C.3}$$

which leads to a variance due to multiple reuse of the data (assuming $\langle \delta p_i^2 \rangle = \frac{p_i}{N}$)

$$\text{Var}_{\text{Slides}}/N = \sum_{j=1}^{D} p_j \left(\sum_{\substack{i=1 \\ i \neq j}}^{D} p_i \right) \left(\sum_{\substack{k=1 \\ k \neq j}}^{D} p_k \right) \tag{C.4}$$

$$= \left(\sum_{j=1}^{D} \sum_{\substack{i=1 \\ i \neq j}}^{D} p_i p_j \right) \left(\sum_{k=1}^{D} p_k \right) - \sum_{j=1}^{D} p_j^2 \sum_{\substack{i=1 \\ i \neq j}}^{D} p_i \tag{C.5}$$

$$= \left(\sum_{j=1}^{D} \sum_{i=1}^{j-1} p_i p_j \right) \left(\sum_{k=1}^{D} p_k \right) + \frac{1}{2} \sum_{j=1}^{D} \sum_{\substack{i=1 \\ i \neq j}}^{D} p_i p_j \left(p_j + p_i + \sum_{\substack{k=1 \\ k \neq i, k \neq j}}^{D} p_k \right) - \sum_{j=1}^{D} \sum_{\substack{i=1 \\ i \neq j}}^{D} p_i p_j^2 \tag{C.6}$$

$$= \left(\sum_{j=1}^{D} \sum_{i=1}^{j-1} p_i p_j \right) \left(\sum_{k=1}^{D} p_k \right) + \frac{1}{2} \sum_{j=1}^{D} \sum_{\substack{i=1 \\ i \neq j}}^{D} \sum_{\substack{k=1 \\ k \neq i, k \neq j}}^{D} p_i p_j p_k. \tag{C.7}$$

This general formula (C.7) is correctly giving back the extra terms in equations (7) and (14) for respectively the 2 and 3 detector case.

References

[1] B. P. Abbott et al. LIGO: the laser interferometer gravitational-wave observatory. *Rep. Prog. Phys.*, 72(7):076901, 2009.

[2] F. Acernese et al. Status of Virgo. *Class. Quantum Grav.*, 25(11):114045, 2008.

[3] B. P. Abbott et al. Search for gravitational-wave bursts in LIGO data from the fourth science run. *Class. Quantum Grav.*, 24(22):5343, 2007.

[4] B. P. Abbott et al. Search for gravitational-wave bursts in the first year of the fifth LIGO science run. *accepted in Phys. Rev. D*, arXiv/0905.0020

[5] B. P. Abbott et al. Search for High Frequency Gravitational Wave Bursts in the First Calendar Year of LIGO's Fifth Science Run. *accepted in Phys. Rev. D*, arXiv/0904.4910

[6] B. P. Abbott et al. Search for gravitational waves from binary inspirals in S3 and S4 LIGO data. *Phys. Rev. D*, 77(6):062002, 2008

[7] B. P. Abbott et al. Search for Gravitational Waves from Low Mass Binary Coalescences in the First Year of LIGO's S5 Data. *Phys. Rev. D*, 79(12):122001, 2009.

[8] B. P. Abbott et al. Search for gravitational waves from low mass compact binary coalescence in 186 days of LIGO's fifth science run *Phys. Rev. D*, 80(4):047101, 2009.

[9] F. Acernese et al. Gravitational wave burst search in the Virgo C7 data. *Class. Quantum Grav.*, 26(8):085009, 2009.

[10] B. Allen. χ^2 time-frequency discriminator for gravitational wave detection. *Phys. Rev. D*, 71(6):062001, 2005.

[11] F. Beauville et al. A comparison of methods for gravitational wave burst searches from LIGO and Virgo. *Class. Quantum Grav.*, 25:045002, 2008.

[12] S. D. Mohanty. Robust test for detecting nonstationarity in data from gravitational wave detectors. *Phys. Rev. D*, 61:122002, 2000.